LETTER

High proton conductivity state of water in nanoporous materials

To cite this article: I. A. Ryzhkin *et al* 2019 *EPL* **126** 36003

A Letters Journal Exploring the Frontiers of Physics

May 2019

EPL, **126** (2019) 36003 www.epljournal.org
doi: 10.1209/0295-5075/126/36003

High proton conductivity state of water in nanoporous materials

I. A. Ryzhkin[1,2], M. I. Ryzhkin[1], A. M. Kashin[2], E. A. Galitskaya[1,2] and V. V. Sinitsyn[1,2]

[1] *Institute of Solid State Physics RAS - 2 Academician Ossipyan Str., Chernogolovka, Moscow District 142432, Russia*
[2] *Inenergy LLC - Elektrodnaya Street 12-1, Moscow, 111524, Russia*

received 10 February 2019; accepted in final form 13 May 2019
published online 18 June 2019

PACS 68.65.-k – Low-dimensional, mesoscopic, nanoscale and other related systems: structure and nonelectronic properties
PACS 87.15.ht – Ultrafast dynamics; charge transfer
PACS 66.10.Ed – Ionic conduction

Abstract – A simple model has been proposed for water confined in nanochannels of a porous material, where the proton conductivity is six orders of magnitude higher than the value for bulk water. The key concept of the model is topological inconsistency of the ice rules with ordering of interface molecules, which results in the formation of excess charge carriers near the interface and in a sharp increase in the proton conductivity of water confined in channels with diameters of about several nanometers as compared to bulk water. Numerical estimates within our model are in quantitative agreement with measured proton conductivities of nanoporous materials with different chemical compositions, degrees of crystallinity, and morphologies of the structure. The model gives a useful scheme for the interpretation of proton transport in confined water and provides recommendations for the fabrication of nanoporous materials with a high proton conductivity.

Introduction. – Water is the most widespread and simultaneously the most mysterious compound on the Earth. It plays a decisive role in many biological, chemical, geological, and technological processes. Its physical properties are extraordinary and are often called anomalies. In particular, water has unusual electrical properties: it is simultaneously an insulator with a high dielectric constant and a conductor where charge carriers are protons [1]. This capability of water to serve as a universal solvent with proton transport determines its role in many biological and technological processes from the synthesis of adenosine triphosphate in biological objects to the generation of electric power in hydrogen fuel elements.

The proton conductivity of pure bulk water is quite low, about $5 \cdot 10^{-6}$ S/m at a temperature of 298 K [2]. At the same time, the conductivity of pure water confined in quasi–one-dimensional channels with a diameter of several nanometers, *e.g.*, in polymer materials such as Nafion is six orders of magnitude higher, about 10 S/m [3]. Why does this difference appear in the proton conductivity between bulk and confined waters? What is the mechanism of the proton conductivity in confined water? What is the maximum proton conductivity possible for confined water? In this work, we formulate a simple theoretical model that naturally answers the above questions, give a theoretical estimate of the maximum proton conductivity of confined water, and discuss its dependence on the area of the internal surface of a porous material and on the temperature. We also present the measured proton conductivities of water in nanoporous materials of various kinds and compare them with theoretical results. In conclusion, we give practice recommendations for the fabrication of proton exchange polymer membranes with a high proton conductivity.

In the next section, we briefly review the mechanism of proton transport in bulk water underlying our model. The main details of this mechanism are well known but are scattered over numerous publications. We include them in this article in order to clarify the presentation. In the third section, which is the central part of this work, we discuss the topological inconsistency of the ice rules, governing the distribution of protons over hydrogen bonds, with any type of proton ordering at the interface of water with the walls of channels. Because of topological inconsistency, excess violations of the ice rules in the bulk of channels are formed and serve as proton charge carriers. The fourth section summarizes the numerical estimates of the proton conductivity, discusses its dependence on the

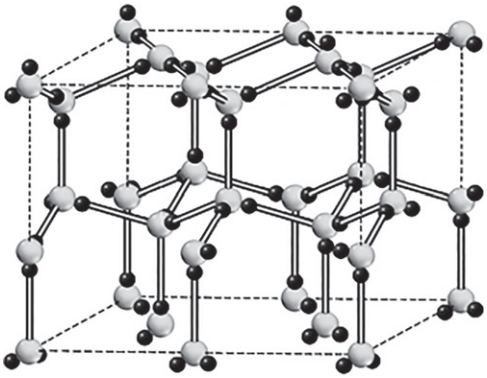

Fig. 1: Fragment of the hexagonal ice lattice, where protons (small black balls) are distributed over hydrogen bonds according to two ice rules.

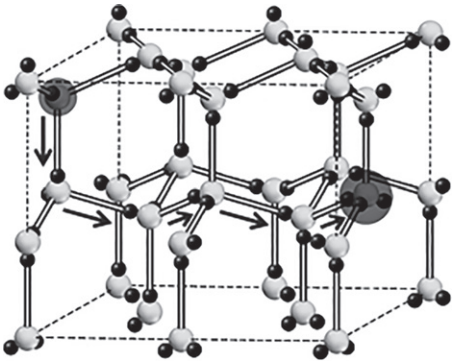

Fig. 2: Formation and motion of ionic defects (two large dark balls). It is shown as the motion of defects polarizes hydrogen bonds.

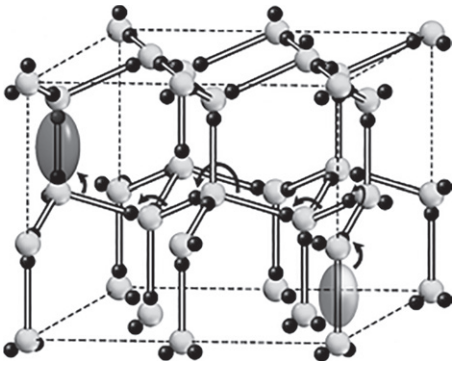

Fig. 3: Formation and motion of bond defects (two large dark ovals, D) and L are bonds with two and zero protons, respectively. It is shown as the motion of the defects polarizes hydrogen bonds.

area of the internal surface, type of ordering, temperature, and describes experimental results, which are in qualitative agreement with our model. Finally, the main features of our model are listed in the fifth section, where we also present a brief recommendation for the fabrication of materials with high proton conductivity.

Proton conductivity mechanism in solid and liquid water. – We first describe the theory of the proton conductivity of solid water. Then, we explain why this theory can be used to describe the proton conductivity of liquid water and, particularly important, of confined liquid water. For definiteness, we consider the most widespread phase of ice called hexagonal ice.

According to [4,5], oxygen ions in this modification form an ordered hexagonal lattice, and protons are distributed over all possible positions on hydrogen bonds according to two ice rules: two protons near each oxygen ion and one proton on each hydrogen bond, see fig. 1.

As seen in this figure, any displacement of a proton to a new position leads to the violation of the ice rules and to an increase in energy; therefore, the proton transport at zero temperature is impossible.

At a finite temperature, violations of the ice rules are possible, and the violations of the ice rules, whose production and motion are shown in figs. 2 and 3, have the lowest excitation energies [6]. Violations of the ice rules or proton point defects are proton charge carriers whose role is similar to the role of electrons and holes in usual electron semiconductors. It is easily seen that the transfer of one proton across a sample occurs through the motion of an H_3O^+ ion in the form of translational jumps of the proton over hydrogen bonds from one molecule to another (see fig. 2) and motion of a D defect through the rotation of a water molecule or the transfer of the proton from one bond to another near one molecule (see fig. 3). Similarly, current can be due to the motion of OH^- and L (oxygen ion with one proton and a hydrogen bond without protons). The described mechanism of proton transport is equivalent to the well-known Grotthuss mechanism [7].

A certain advantage of the description of proton transport in terms of defects is as follows. The number of defects under normal conditions is small and they can be treated as noninteracting particles, whereas the concentration of water molecules is much higher and they strongly interact with each other by means of the ice rules. Thus, violations of the ice rules serve as classical quasiparticles, which are very useful for the description of proton transport.

The microscopic theory of proton transport in ice based on the motion of proton point defects was developed by Jaccard [8] and substantially improved by Hubmann [9]. Further, for convenience, we briefly present the main concepts and results of the theory in notation from [10]. As seen in figs. 2 and 3, the motion of defects through the lattice is responsible for the polarization of bonds, which can be described by a vector parameter called configuration vector $\mathbf{\Omega}$. The configuration vector $\mathbf{\Omega}$ is related to the defect flux densities $\mathbf{j}_\alpha$ as

$$\mathbf{\Omega}(t) - \mathbf{\Omega}(0) = \int_0^t (\mathbf{j}_1 - \mathbf{j}_2 - \mathbf{j}_3 + \mathbf{j}_4)\mathrm{d}t', \qquad (1)$$

where t is the time and $\mathbf{j}_\alpha$ with $\alpha = 1, 2, 3$, and 4 are fluxes of H_3O^+, OH^-, D and L defects, respectively. At the same

time, the configuration vector contributes to the defect fluxes, which can be represented in the form

$$\mathbf{j}_\alpha = \frac{\sigma_\alpha}{e_\alpha^2}(e_\alpha \mathbf{E} - \eta_\alpha \Phi \mathbf{\Omega}). \quad (2)$$

Here, $\sigma_\alpha = |e_\alpha|\mu_\alpha n_\alpha$ are the partial conductivities of defects, where μ_α are their mobilities, $e_{1,2} = \pm 0.62e$ and $e_{3,4} = \pm 0.38e$ are their effective charges; $\mathbf{E}$ is the electric-field strength; coefficients η_α are $1, -1, -1$, and 1 for $\alpha = 1, 2, 3$, and 4, respectively; and $\Phi = (8/\sqrt{3})r_{OO}k_BT$, where r_{OO} is the length of hydrogen bonds. Concentrations of defects are determined by the Arrhenius laws $n_\alpha \propto \exp(-E_\alpha/2k_BT)$ and the conductivity of ice is low because of noticeable activation energies 1.2 and 0.68 eV of ionic and bond defects, respectively.

The expression for conductivity can be obtained as follows. In the Fourier representation, the system of equations. (1), (2) is a system of linear algebraic equations. To find the conductivity we first exclude the flux densities $\mathbf{j}_\alpha$ from this system and find the expression for the configuration vector $\mathbf{\Omega}$ in terms of the electric field $\mathbf{E}$. Then we substitute this expression into the equations for the flux densities and find them as functions of only the electric field. And finally, using the equation for electric current density $\mathbf{j} = \sum_{\alpha=1}^{4} e_\alpha \mathbf{j}_\alpha$ we find it as a function of the electric field, that is we find the conductivity. Omitting the rather cumbersome calculations, we present the final expression for the proton conductivity in the following form:

$$\sigma(\omega) = \sigma_1 + \sigma_2 + \sigma_3 + \sigma_4 - \frac{\Phi\tau[(\sigma_1+\sigma_2)/e_1 - (\sigma_3+\sigma_4)/e_3]^2}{1 - i\omega\tau}, \quad (3)$$

$$1/\tau = \Phi[(\sigma_1+\sigma_2)/e_1^2 + (\sigma_3+\sigma_4)/e_3^2]. \quad (4)$$

For ice under normal conditions, $\sigma_1 + \sigma_2 \ll \sigma_3 + \sigma_4$ and it is easy to obtain the following expressions for the low-frequency (high-frequency) conductivity, relaxation time, and low-frequency dielectric constant:

$$\sigma(\omega \to 0) \approx \frac{e^2}{e_1^2}(\sigma_1+\sigma_2), \qquad \sigma(\omega \to \infty) \approx (\sigma_3+\sigma_4), \quad (5)$$

$$\tau \approx \frac{e_3^2}{\Phi(\sigma_3+\sigma_4)}, \qquad \epsilon \approx \epsilon_\infty + \frac{4\pi e_3^2}{\Phi}. \quad (6)$$

Here, $\epsilon_\infty = 3.2$ is the high-frequency dielectric constant due to ions and electrons, and the low-frequency dilectric permittivity is defined as $\epsilon(\omega) = -4\pi\sigma(\omega)/i\omega$ at $\omega \to 0$.

The physical meaning of the above results is as follows. Majority carriers with a higher partial conductivity, *i.e.*, D and L bond defects first respond to the applied electric field. As a result, the polarization of hydrogen bonds appears in the relaxation time τ and is described by the dielectric constant ϵ. Further motion of bond defects becomes impossible because of the polarization of bonds (see figs. 2 and 3). However, in this polarization state, minority carriers, *i.e.*, H_3O^+ and OH^- ionic defects can move and this motion ensures a direct current. Thus, the high-frequency conductivity and time relaxation are determined by bond defects, whereas the low-frequency conductivity or the rate of proton transport is determined by ionic defects. The described picture corresponds to pure ice under normal conditions. In impurity ice or at a high pressure, the relation between partial conductivities can be significantly different, but eqs. (3) and (4) are always applicable. Numerical values of the effective charges, activation energies of proton point defects, mobilities, and mobility activation energies are presented in [1]. The use of these values together with eqs. (3)–(5) provides the complete description of proton transport in ice in quantitative agreement with the results of numerous experiments.

Beginning the description of the proton conductivity of water, we first note that the system of hydrogen bonds in a liquid state at not too high temperatures is largely preserved. In particular, according to [11], about 90 percent of hydrogen bonds remain in bulk water at a temperature of 273 K immediately after melting. The conservation of hydrogen bonds in confined water is more probable [12–16] even at the temperatures at which bulk water boils. According to another approach, liquid water consists of small ice clusters separated by thin layers of the liquid phase [17,18].

In [2,19,20], it was shown that the Jaccard theory can be modified within any of these approaches to describe the proton conductivity of liquid water. Modification includes the reduction of the formation energy of proton point defects because of a first-order phase transition in the proton subsystem of ice [11]: the formation energies of ionic and bond defects for liquid water are 0.79 and 0.14 eV, respectively. This means that for water one can use all the formulas of the Jaccard theory (1)–(6) using only these new values for the activation energies of defects (see also [20]). The melting also affects the mobilities of defects: the mobilities of ionic defects decrease noticeably, whereas the mobilities of bond defects increase in view of partial destruction of the tetrahedral structure. The relaxation time τ can be considered as the characteristic lifetime of a hydrogen bond and it can be estimated as 10–100 ps depending on the mobilities of bond defects in the liquid state.

According to the above discussion, the Jaccard theory can be used even for the description of proton transport in bulk water, where the transition to the liquid state of hydrogen bonds is accompanied by a noticeable (about 10 percents, see above) destruction of the oxygen lattice. The destruction of the oxygen lattice in water confined in nanochannels of porous materials will be smaller and the application of the Jaccard theory is even more justified.

Topological inconsistency of ice rules with interface ordering. – As mentioned above, the conductivity of water is low primarily because the concentration of violations of the ice rules, which are charge carriers, is low. Obvious methods for increasing concentrations of defects are an increase in the temperature and introduction of

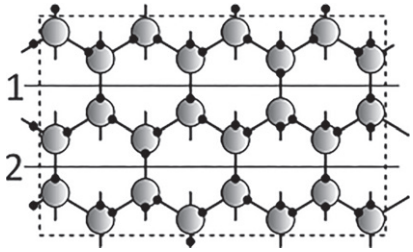

Fig. 4: Fragment of the hexagonal ice lattice, where protons (small black circles) are distributed according to the ice rules, the hexagonal axis is vertical.

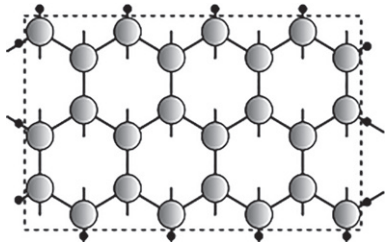

Fig. 5: Fragment of the hexagonal ice lattice with outward ordering of protons; inner protons are not shown. The confined surface is shown by the dashed line.

certain impurities. A less obvious method is an increase in the area of the interface of water with walls of the confining material. This can be implemented by introduction of water into nanoporous materials with a large internal surface. The reason why the interface leads to an increase in the concentration of violations of the ice rules, is the topological inconsistency between the ice rules and any type of surface ordering. Surface ordering at any orientation of interface molecules (with protons toward or outward the interface) should generate violations of the ice rules near the interface.

To demonstrate this, we consider the fragment of the ice lattice shown in fig. 4. We show that vertical bonds intersected by planes 1 and 2 separating one basal plane should have the same polarization (the same number of protons above the planes) if the ice rules are satisfied.

Let $2N$ be the number of oxygen sites between planes 1 and 2, and p be the probability of the vertical bond (intersected by plane 1) with the proton below plane 1. In this case, when the ice rules are satisfied, the number of protons between the planes is $4N$, among which $3N$ protons are on inclined bonds. Then, the number of protons on vertical bonds intersected by plane 1 and below this plane is pN, and the number of protons on vertical bonds intersected by plane 2 and above this plane is $4N - 3N - pN = (1 - p)N$. Finally, the number of protons on vertical bonds intersected by plane 2 and below this plane is $N - (1 - p)N = pN$. The last statement means that vertical bonds intersected by planes 1 and 2 have the same polarization, and this conclusion obviously concerns all vertical bonds. However, in this case, the upper and lower faces of the sample should have the same polarization, *e.g.*, outward protons on the upper face and inward protons on the lower face, which is physically contradictory for $p \neq 1/2$.

The only method to solve this contradiction is to introduce violations of the ice rules into the bulk of the crystal: these violations make the presented proof impossible. If the interaction with the surface is such that a certain ordering exists at surface, that is $p \neq 1/2$, this interaction certainly generates violations of ice rules inside the sample.

The indicated inconsistency between the ice rules and any ordering at the interface is topological. To demonstrate this, we consider the ice sample shown in fig. 5 and assume for definiteness that protons are oriented toward the outer surface. According to the Gauss theorem [21], the flux of dipole momentum $\mathbf{P}$ through the confined surface S is related to the polarization charge Q in the bulk:

$$\oint_S \mathbf{P} \cdot \mathrm{d}\mathbf{s} = -\frac{Q}{4\pi}. \tag{7}$$

The latter means that violations of the ice rules with effective charges should inevitably exist inside the sample.

Finally, we note that violations of the ice rules are always produced pairwise as shown in figs. 2 and 3. The appearance of surface polarization means that either a D defect (at the outward polarization of protons) or an L defect (at the inward polarization of protons) reaches the surface. At the same time, a bond defect of the opposite type remains in the bulk. The surface polarization can also be due to the confining material, which can yield protons on dangling bonds or take protons from these bonds. In this case, H_3O^+ and OH^- ionic defects will be produced in the sample, respectively.

Thus, we have shown that the polarization of outer molecules inevitably means the existence of violations of the ice rules in the bulk of the sample, and the number of these violations is determined by the number of surface molecules and the degree of surface ordering. The fraction of surface molecules for bulk samples is obviously negligibly small and the indicated source of proton current carriers is insignificant. However, this source of proton current carriers can become major for one- and two-dimensional water or water in a nanoporous material with a huge internal surface.

Topological reasons indicate that proton point defects additional to thermally excited defects should exist. A particular type of additional defects, as well as a change in the conductivity, depends on the type of the material of channel walls and the type of interaction of water molecules with walls. The following typical cases can be listed. In the first case, protons on surface bonds come from the bulk and additional bond defects of the L type appear in confined water. Their number is given by the formula $N_L = (p - 1/2)N_S$, where p and N_S are the degree of ordering and the number of surface bonds, respectively. If this number becomes noticeable as compared

to the number of thermally excited bond defects, a certain increase in the high-frequency conductivity, which is determined by bond defects, should be expected. In this case, the low-frequency proton conductivity will slightly decrease because of the destruction of the system of hydrogen bonds and a decrease in the mobility of ionic defects, as at the melting of ice. This remark concerns the low-frequency conductivity measured at blocking contacts (without exchange by protons). At the same time, if protons can be injected from contacts, each injected proton eliminates an L defect and creates a H_3O^+ defect, which contributes to an increase in the transport proton conductivity.

In the second case, the interaction of the material of walls with interface water molecules is such that dangling bonds are proton-free. In this case, additional D defects, which have a very low mobility, appear in confined water. In this case, both the low- and high-frequency conductivities hardly change.

In the most interesting third case, proton-free sites on dangling (surface) bonds are occupied by protons from the material of walls of channels; *i.e.*, surface ordering is due to external protons. In this case, additional H_3O^+ ionic defects appear in water; these defects determine the low-frequency conductivity of water and have the highest mobility. The concentration of additional ionic defects is bounded from above by a value of unity and their concentration in pure water is near 10^{-7}. This means that an increase in the transport proton conductivity by many orders of magnitude can be in principle expected. This third case has the following analog in the physics of semiconductors. The introduction of a large number of donor impurities (sources of electrons) into an intrinsic semiconductor (analog of pure water) can give a degenerate semiconductor with a high electron conductivity and with the Fermi level in the conduction band. This state of the semiconductor is equivalent to a metallic state. In view of this analogy, the state of water with a large number of injected H_3O^+ ionic defects can be called the metallic state of water. In the next section, we compare our conclusions with experimental results.

Comparison with experimental results. – We compare the above estimates with experimentally measured conductivities of water confined in pores of nanoporous materials of different types: carbon nanotubes, silica-based nanoporous materials (initial and modified materials such as MCM-41 and SBA-15), and Nafion perfluorinated polymer membranes. The diameters of channels in these materials can be about several nanometers. They are widely used, the technology of their fabrication is well developed, and we expect that they can implement all above-discussed methods for proton ordering of interface water because of their chemical composition. Furthermore, silica-based nanoporous materials are often modified in an acid medium in order to produce acid groups, which can be donors of protons, on channel walls. This means that these modified materials can implement intermediate types of proton ordering: ordering owing to the orientation of water molecules and ordering owing to proton doping.

We begin with experimental results for the measured proton conductivity in carbon nanotubes. Carbon nanotubes do not contain protons, and this means that interface molecules are oriented with protons either toward (first case) or outward (second case) the walls of the channel. An increase in the relative concentration of bond defects is given by the formula

$$x_L \simeq \frac{N_{D,L}}{2N_{H_2O}} = \frac{(S/a^2)(p-1/2)}{2V/a^3} = 2\frac{a}{d}(p-1/2), \quad (8)$$

where a is the distance between water molecules and d, S, and V are the diameter of the cylindrical tube, the internal surface area, and free volume of the porous material, respectively. At the diameter of 4 nm and $p = 1$, the additional concentration is about $x_L \simeq 0.07$, which approximately corresponds to the concentration in bulk water. As shown above, a certain (less than an order of magnitude) increase in the high-frequency conductivity should be expected in this case, and a certain increase in the transport conductivity (easier injection) is possible if interface water molecules are oriented with protons toward the interface. Otherwise, low-mobility D defects are injected and a decrease in both the high- and low-frequency conductivities is most probable.

The experimentally determined low-frequency conductivity [22] of water in carbon nanotubes is about $1.6 \cdot 10^{-6}$ and $9.1 \cdot 10^{-6}$ S/m for tubes with a diameter of 1.4 and 0.7 nm, respectively. The first value is in agreement with our predictions: it is lower than the proton conductivity of bulk water. The second value is twice as high as the proton conductivity of bulk water, which can be explained by an increase in the mobility of ionic defects in the interface water layer. Indeed, the walls of the channel with a diameter of 0.7 nm are coated with only one monolayer of water molecules, and the situation in this case is closer to the model of single-file water, which is not described within our macroscopic approach. Numerical results for this model confirm an increase in the mobility of ionic defects, which can explain an increase in the proton conductivity with a decrease in the diameter of the carbon nanotube [23].

Now we consider nanoporous silica-based materials such as initial and modified MCM-41 and SBA-15. The interaction of water molecules with walls in pores of such materials is significantly more complex because Si–O–H hydroxyl groups are formed on the surface of SiO_2 and their concentration is close to unity [24,25]. Hydroxyl groups can be donors of protons for water, thus increasing the concentration of mobile ionic defects in water. However, this process requires an energy close to the formation energy of ionic defects in bulk water. Consequently, proton doping by hydroxyl groups hardly changes

the proton conductivity of water. Nevertheless, the low-frequency proton conductivity of water in silica-based materials can be significantly increased through modification by the SO_3H sulfonic group [26–30].

Modification can be performed by two methods: i) processing of a finished porous material (crafting) and ii) addition of sulfonic acid at the stage of synthesis of the porous material (co-condensation) [28]. The latter method makes it possible to obtain materials with a higher proton conductivity probably because the resulting concentration of sulfonic groups in this case is higher (see also perfluorinated polymer materials). Let us assume that the relative surface concentration of the Si–SO_3H sulfonic group is about 0.1. Then the relative concentration of doped positive ionic defects will be defined by the equation (see the notation after formula (8))

$$x_+ = 0.1\frac{S/a^2}{V/a^3} = 0.1\frac{\pi d/a^2}{\pi d^2/4a^3} = \frac{0.4a}{d}. \tag{9}$$

Taking $a = 0.28\,\mathrm{nm}$, $d = 2\,\mathrm{nm}$, the diffusion coefficient $D_+ = 4 \cdot 10^{-9}\,\mathrm{m^2/s}$ (as in bulk water), we come to the following estimation of conductivity:

$$\sigma = e_1^2 D_+ x_+ N_0/kT \approx 16\,\mathrm{S/m}, \tag{10}$$

where N_0 is the volume concentration of water molecules. This value is in qualitative agreement with the results obtained in [27,29,30] and a minor quantitative difference can be attributed to a lower concentration of sulfonic groups as compared to the value used for the estimate.

We now discuss the measured proton conductivities of Nafion perfluorinated sulfonic polymer membranes. The structure of channels in this type of membranes is widely studied, but the final model has not yet been developed. The structure and diameters of channels in this type of materials obviously depend on the technology of their fabrication and additional processing for an increase in the proton conductivity. The model of cavities with a diameter of about 4 nm connected by channels with a diameter of about 1 nm [31] and the model of cylindrical channels with a diameter in this range [32] are the most widespread models. Both models imply that side branches ending with a sulfonic group exist on the walls of pores or channels. The explanation of a high proton conductivity in these materials is the same as for modified silica-based materials: protons of sulfonic groups with a certain activation energy are transferred to water and ensure its high proton conductivity.

The low-frequency conductivity can be theoretically estimated as follows. A spherical cavity 4 nm in diameter in the Gierke model [31] contains about 1000 water molecules. The number of side sulfonic branches in this case is approximately 30. Then, the relative concentration of positive ionic defects is 0.03. Using the same value for the diffusion coefficient of H_3O^+ defects as in (10), we obtain a low-frequency conductivity of 9 S/m. This value very accurately agrees with the results from [33] and is in qualitative agreement with the results of other experimental works [34–37].

Conclusions. – To summarize, the proposed model has been qualitatively confirmed by experimental results and provides an appropriate scheme for understanding the mechanism of the proton conductivity of water confined in nanochannels of porous materials of different types.

The main characteristics and fundamentally new features of our model are as follows. First, proton transport in confined water is described within the slightly modified Jaccard theory, which quantitatively reproduces proton transport in ice. Second, the analysis of the inconsistency of proton ordering at the interface with the ice rules governing the distribution of protons over hydrogen bonds makes it possible to understand the mechanism of production of additional charge carriers in confined water. Third, in contrast to other theoretical models involving only one type of carriers (ionic defects), we consider two types of carriers (ionic and bond defects), which allows the adequate description of proton transport in nanoporous materials of different types. It is noteworthy that the frequency dependence of the proton conductivity can in principle be predicted within our model with two types of carriers.

We also note that the analysis of numerical estimates and experimental results indicates that the transport proton conductivity of water in a nanoporous material can be increased by increasing the concentration of the proton complexes on the surface of channel walls and by decreasing the diameter of channels. According to our estimates, a transport proton conductivity of about 160 S/m can be achieved at the extremely high concentration of proton centers, minimum possible diameter of channels, and the mobility of ionic defects characteristic for bulk water. A further increase in the proton conductivity can be achieved only by increasing the mobility of ionic defects in view of proton quantum effects.

In conclusion, we describe the relationship of this work with the recently published one given in ref. [38]. As was shown in [38], the most interesting results for conductivity of confined water arise when the channel diameters are of the order of intermolecular distances, which makes the continuous model used there inapplicable. For this reason, in this work, we do not use a continuous approach and do not calculate the dependence of the concentrations on the distances from the channel walls. Instead, we estimate the total number of current carriers generated by the interaction of water molecules with the walls of channels. That makes such an approach applicable even for the narrowest channels.

Besides that, here we provide a detailed discussion of the experimental results and demonstrate the topological character of incompatibility between ice rules and any ordering at the surface. Exactly the topological nature of this incompatibility underlies its wide applicability. For example, in [39–41], this incompatibility was used to explain a quasi-liquid layer on the free surface of ice. It

can be said that we use the generalization of the approach from [39–41] to describe the water confined in nanoporous materials.

* * *

We are grateful to A. V. Klyuev for figures and stimulating discussions. This work was supported in part by the Russian Foundation for Basic Research (grant No. 17-02-00512).

REFERENCES

[1] Petrenko V. F. and Whitworth R. W., *Physics if Ice* (Oxford University Press, New York, USA) 1999.
[2] Artemov V. G., Ryzhkin I. A. and Sinitsyn V. V., *JETP Lett.*, **102** (2015) 41.
[3] Saito M., Hayamizu K. and Okada T., *J. Phys. Chem.*, **109** (2005) 3112.
[4] Bernal J. D. and Fowler R. H., *J. Chem. Phys.*, **1** (1933) 515.
[5] Pauling L., *J. Am. Chem. Soc.*, **57** (1935) 2680.
[6] Bjerrum N., *K. Dan. Vidensk. Selsk. Mat.-fys. Med.*, **27** (1951) 1.
[7] Grotthuss C. J. T., *Ann. Chim.*, **LVIII** (1806) 54.
[8] Jaccard C., *Phys. kondens. Materie*, **3** (1964) 99.
[9] Hubmann M., *Z. Phys. B*, **32** (1979) 127.
[10] Petrenko V. F. and Ryzhkin I. A., *J. Phys. Chem. A*, **115** (2011) 6202.
[11] Ryzhkin M. I., Klyuev A. V., Sinitsyn V. V. and Ryzhkin I. A., *JETP Lett.*, **104** (2016) 248.
[12] Sedlmeier F., Janecek J., Sendner C. and Bocquet L., *Biointerphases*, **3** (2008) 23.
[13] Corsetti F., Matthews O. and Artacho E., *Sci. Rep.*, **6** (2016) 18651.
[14] Wei X., Miranda P. B., Zhang C. and Shen Y. R., *Phys. Rev. B*, **66** (2002) 085401.
[15] Strazdaite S., Versluis J., Backus E. H. G. and Bakker H. J., *J. Chem. Phys.*, **140** (2014) 054701.
[16] Kofinger J., Hummer G. and Dellago C., *Proc. Natl. Acad. Sci. U.S.A.*, **105** (2008) 13218.
[17] Rontgen W. C., *Ann. Phys. Chem.*, **45** (1892) 91.
[18] Nemethy G. and Scheraga H. A., *J. Chem. Phys.*, **36** (1962) 3382.
[19] Artemov V. G. and Volkov A. A., *Ferroelectric*, **466** (2014) 158.
[20] Klyuev A. V., Ryzhkin I. A. and Ryzhkin M. I., *JETP Lett.*, **100** (2014) 604.
[21] Jackson J. D., *Classical Electrodynamics* (John Wiley and Sons, New York, USA) 1999.
[22] Tunuguntla R. H., Allen F. I., Kim K., Belliveau A. and Noy A., *Nat. Nanotechnol.*, **11** (2016) 639.
[23] Dellago C., Naor M. M. and Hummer G., *Phys. Rev. Lett.*, **90** (2003) 105902.
[24] Pelmenschikov A. G., Morosi G. and Gamba A., *Nuovo Cimento D*, **19** (1997) 1749.
[25] Gaigeot M. P., Sprik M. and Sulpizi M., *J. Phys.: Condens. Matter.*, **24** (2012) 124106.
[26] Marshall R., Bannat I., Caro J. and Wark M., *Microporous Mesoporous Mater.*, **99** (2007) 190.
[27] Marshall R., Rathousky J. and Wark M., *Chem. Mater.*, **19** (2007) 64501.
[28] Hoffmann F., Cornelius M., Morell J. and Froba M., *Angew. Chem., Int. Ed.*, **45** (2006) 3216.
[29] Fujita S., Koiwai A., Kawasumi M. and Inagaki S., *Chem. Mater.*, **25** (2013) 1584.
[30] Colomer M. T., Rubio F. and Jurado J. R., *J. Power Sources*, **167** (2007) 53.
[31] Gierke T. D., Munn G. E. and Wilson F. C., *J. Polym. Sci. B: Polym. Phys. Ed.*, **19** (1981) 1687.
[32] Schmidt-Rohr K. and Chen Q., *Nat. Mater.*, **7** (2008) 75.
[33] Mugtasimova K. R., Melnikov A. P., Galitskaya E. A., Kashin A. M., Dobrovolskiy Yu. A., Don G. M., Likhomanov V. S., Sivak A. V. and Sinitsyn V. V., *Ionics*, **24** (2018) 3897.
[34] Dong B., Gwee L., de la Cruz D. S., Winey K. I. and Elabd Y. A., *Nano Lett.*, **10** (2010) 3785.
[35] Yang C., Srinivasan S., Bocarsly A. B., Tulyani S. and Benziger J. B., *Nafion/ZP Compos. Membr.*, **9** (2003) 15.
[36] Artemov V. G., *Meas. Sci. Technol.*, **28** (2017) 014013.
[37] Trigg E. B., Gaines T. W., Marechal M., Moed D. E., Rannou P., Wagener K. B., Stevens M. J. and Winey K. I., *Nat. Mater.*, **17** (2018) 724.
[38] Ryzhkin M. I., Ryzhkin I. A., Kashin A. M., Galitskaya E. A. and Sinitsyn V. V., *JETP Lett.*, **108** (2018) 596.
[39] Fletcher N. H., *Philos. Mag.*, **7** (1962) 255.
[40] Fletcher N. H., *Philos. Mag.*, **8** (1963) 1425.
[41] Fletcher N. H., *Philos. Mag.*, **18** (1971) 3887.